Acta Cryst. (1997). D**53**, 724–733

Comparative Analysis of Thaumatin Crystals Grown on Earth and in Microgravity

JOSEPH D. NG,[a] BERNARD LORBER,[a] RICHARD GIEGÉ,[a]* STANLEY KOSZELAK,[b] JOHN DAY,[b] AARON GREENWOOD[b] AND ALEXANDER MCPHERSON[b]

[a]*UPR 9002, Structure des Macromolécules Biologiques et Mécanismes de Reconnaissance, Institut de Biologie Moléculaire et Cellulaire du CNRS, 15 rue René Descartes, F-67084 Strasbourg, France, and* [b]*University of California, Riverside, Department of Biochemistry, Riverside, CA 92521, USA. E-mail: giege@ibmc.u-strasbg.fr*

(*Received 3 February 1997; accepted 8 May 1997*)

Abstract

The protein thaumatin was studied as a model macromolecule for crystallization in microgravity-environment experiments conducted on two US Space Shuttle missions (USML-2 and LMS). In this investigation, we have evaluated and compared the quality of space- and earth-grown thaumatin crystals using X-ray diffraction analyses, and characterized them according to crystal size, diffraction resolution limit and mosaicity. Two different approaches for growing thaumatin crystals in the microgravity environment, dialysis and liquid–liquid diffusion, were employed as a joint experiment by our two investigative teams. Thaumatin crystals grown in a microgravity environment were generally larger in volume and the total number of crystals was less, relative to crystals grown on earth. They diffracted to significantly higher resolution and with improved diffraction

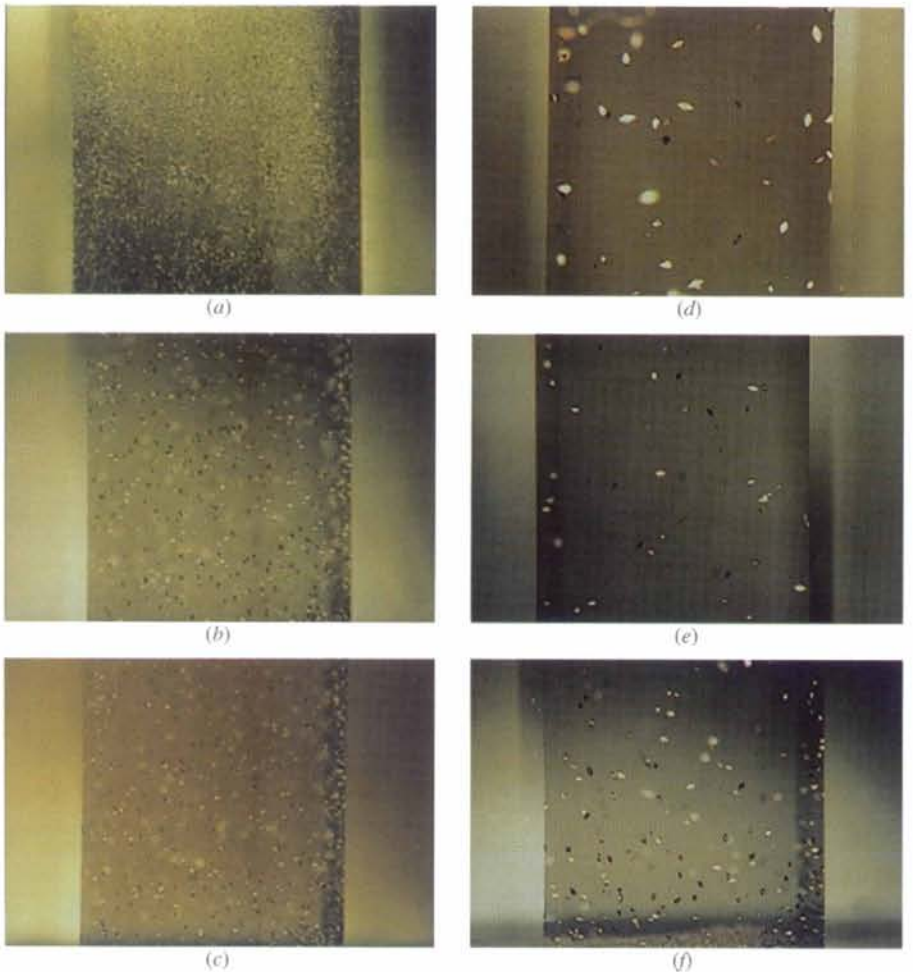

Fig. 1. Comparison of thaumatin crystals grown on earth, (*a*)–(*c*), with those grown in microgravity, (*d*)–(*f*) (corresponding to reactors 2, 5 and 4, respectively, as listed in Table 2). Only the protein-containing chambers of the reactors are shown and those seen here represent typical observations of the 188 µl volume APCF dialysis reactors with low concentrations of thaumatin (6 mg ml^{-1}). Numerous and extremely small crystals are observed in the ground controls compared with only a few larger crystals in space. The average longest dimensions measured for crystals grown on earth and in space were 0.1 and 0.5 mm, respectively. All images are at the same magnification.

© 1997 International Union of Crystallography
Printed in Great Britain – all rights reserved

properties, as judged by relative plots of I/σ *versus* resolution. The mosaicity of space-grown crystals was significantly less than that of crystals grown on earth. Increased concentrations of protein in the crystallization chambers in microgravity led to larger crystals. The data presented here lend further support to the idea that protein crystals of improved quality can be obtained in a microgravity environment.

1. Introduction

Previous experiments have shown that, in at least some cases, macromolecular crystals of improved quality can be grown in a microgravity environment as obtained, for example, in the US Space Shuttle, the Russian Space Station Mir, or unmanned satellites (DeLucas *et al.*, 1989; Asano, Fujita, Senda & Mitsui, 1992; Day & McPherson, 1992; Koszelak, Day, Leja, Cudney & McPherson, 1995; Long *et al.*, 1996; Pan, Niu, Gui, Zhou & Bi, 1996). Presently, the most extensively used facility for such experiments is the Advanced Protein Crystallization Facility (APCF) designed by the European Space Agency (ESA) (Snyder, Fuhrmann & Walter, 1991; Bosch, Lautenschlager, Potthast & Stapelmann, 1992). This system allows crystallization to proceed by vapor diffusion, batch, dialysis and free-interface diffusion methods and provides limited video recording of some experiments as they proceed in space.

On the Space Shuttle missions designated United States Microgravity Laboratory-2 (USML-2, October 1995) and Life and Microgravity Sciences (LMS, June 1996), joint experiments were carried out by our French (Strasbourg) and American (Riverside) groups based on the crystallization of the protein thaumatin. Using common protein, buffer and precipitant solutions, thaumatin was crystallized at a variety of protein concentrations using two different approaches: dialysis and liquid–liquid diffusion. Following retrieval of the samples, microscopy and X-ray analyses were carried out on the crystals grown in microgravity and on control crystals prepared in parallel on earth. Of particular interest to us were (i) the relevance of the choice of methodology, (ii) the influence of protein concentration on crystal size, and (iii) the results of a quantitative comparison of the microgravity-grown crystals with those produced on earth.

2. Materials and methods

2.1. *Protein and chemicals*

Thaumatin was purchased from Sigma (St Louis, MO). A single batch (Cat. No. T-7638, Lot 108 F0299) of dry protein powder was used. The protein was dissolved either in a buffer prepared with 0.1 *M N*-(2-acetamido)-2 iminodiacetic acid (ADA) (Sigma, Cat. No. A-9883, Lot 92 H5635), adjusted to pH 6.5 with NaOH, or in water (see Table 1). For crystallization, the precipitant stock solution was 1.6 *M* sodium DL-tartaric acid (Sigma, Cat. No. T-5259, Lot 101 H0695) in 0.1 *M* ADA titrated with NaOH to pH 6.5. All solutions were prepared with

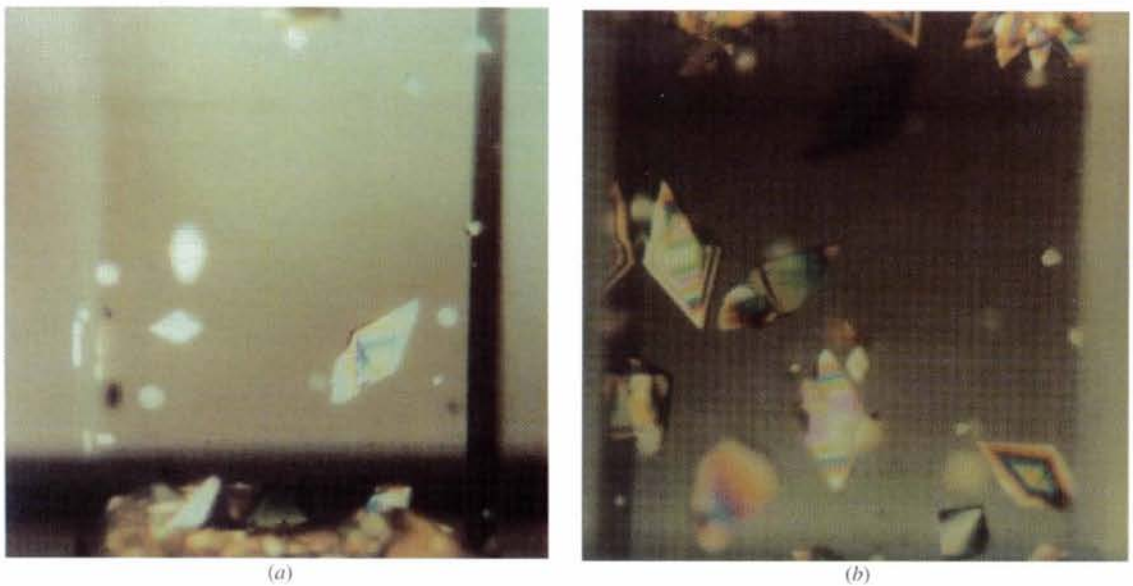

(*a*) (*b*)

Fig. 2. Earth-grown thaumatin crystals, (*a*), compared with space-grown crystals, (*b*), in a 67 µl volume APCF dialysis reactor (Table 2, reactor 1). The images show the protein chambers containing crystals grown at high concentrations of thaumatin (20 mg ml^{-1}). Crystals grown on earth ranged in size from 0.1 to 1.2 mm in the longest dimension and most of the crystals are seen to have formed a sediment on the bottom membrane. Space-grown crystals, on the other hand, grew with a size range of 0.5 to 1.7 mm from apex to apex. Fewer and larger crystals were observed in this space reactor than in the corresponding earth control reactor.

ultrapure sterile water (Fresenius, Louviers, France) and sterilized by filtration through membranes of 0.22 μm pore size (Millipore, Millex).

A concentrated stock solution of thaumatin was freshly prepared by adding 1 ml of ADA buffer, pH 6.5, to 100 mg of protein powder. After dissolution, the solution was centrifuged for 20 min at 15 000*g*. The supernatant was filtered through 0.22 μm ultrafree low-binding membranes (Millipore, Cat. No. UFC3 0 GV 00). The protein concentration was calculated from the UV absorbance of a 1/250 dilution using a molar extinction coefficient of 28 270 (based on the tryptophan and tyrosine content). Buffer and tartrate solutions used by both laboratories were made in Strasbourg and divided between investigators.

2.2. *Instrumentation and crystallization conditions*

The APCF has been described previously (Snyder *et al.*, 1991; Bosch *et al.*, 1992) and, indeed, successful experiments with other proteins and viruses have been reported (*e.g.* Koszelak *et al.*, 1995; Snell *et al.*, 1995; Chayen, Gordon & Zagalsky, 1996). An APCF unit has provision for a total of 48 individual reactors maintained at constant temperature [295.0 (1) K in this case] from the time of loading, for the duration of the mission, to analysis. Both the dialysis and the free-interface diffusion cell types are activated by a 90° rotation of a stopcock valve that establishes continuity between protein and precipitant chambers. For dialysis, a semipermeable membrane separates the two chambers. In experiments conducted on USML-2, the Strasbourg group used five dialysis crystallization reactors and the Riverside group three free-interface diffusion reactors. For LMS, the Strasbourg group used two reactors of the dialysis type and the Riverside group two of the liquid–liquid diffusion type. The contents of the reactors and the crystallization conditions are described in Table 1. Methodological aspects of the pre-flight ground experiments and the optimal use of the APCF reactors during

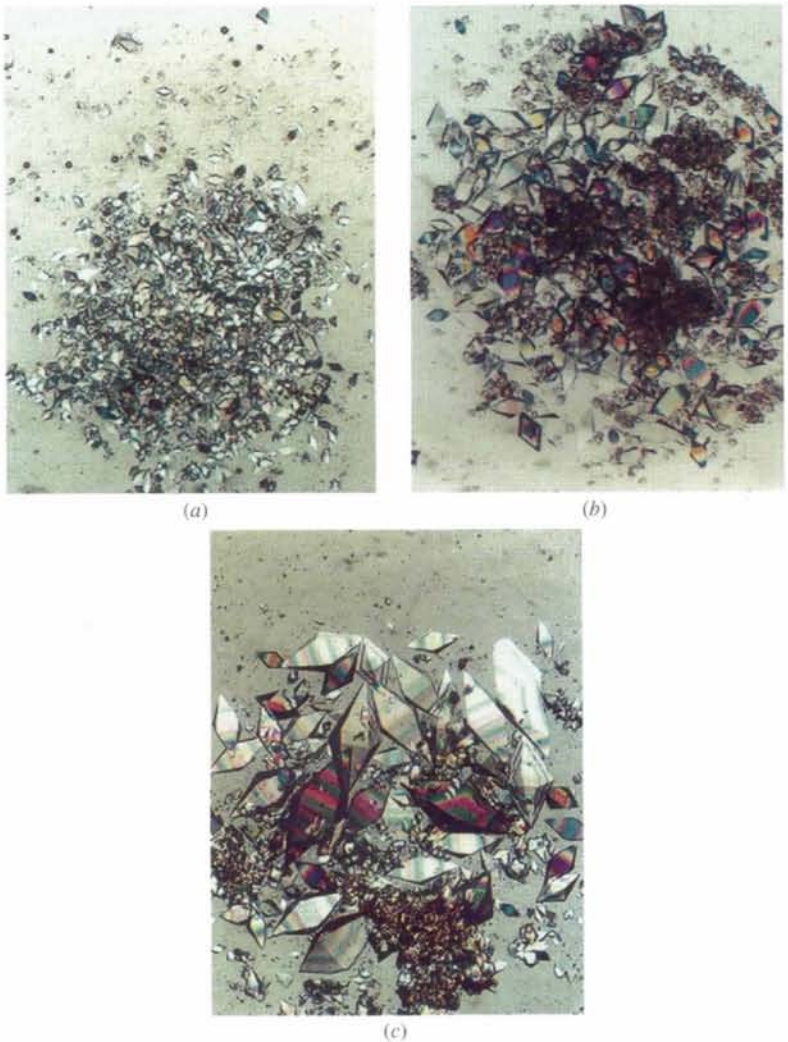

(*a*) (*b*) (*c*)

Fig. 3. Thaumatin microgravity-grown crystals obtained at three different protein concentrations, (*a*) 7, (*b*) 17 and (*c*) 35 mg ml^{-1}, by free-interface diffusion (Table 1, reactors 8–10). Each image is at the same magnification. The largest crystals measure more than 2 mm in the longest dimension and were those used for X-ray data collection.

Table 1. *Contents of APCF reactors*

Chambers exist for both APCF dialysis (D) and free-interface diffusion (FID) reactors; the buffer chamber is absent in the FID cell. Solution *A* is 0.1 *M* ADA buffer and 0.20 *M* sodium tartrate, pH 6.5. Solution *B* is 0.1 *M* ADA buffer and 0.95 *M* sodium tartrate, pH 6.5. Ground reactors were prepared in parallel with exactly the same contents as reactors 1–7.

			Reactor chambers								
			Protein			Buffer		Piston		Salt	
Reactor No.	Flight	Type	Protein conc. (mg ml^{-1})	Buffer	Volume (µl)	Buffer	Volume (µl)	Buffer	Volume (µl)	Buffer	Volume (µl)
1	USML-2	D	6	*A*	188	*B*	59	*B*	246	*B*	295
2	USML-2	D	6	*A*	188	*B*	59	*B*	246	*B*	295
3	USML-2	D	6	*A*	188	*B*	59	*B*	246	*B*	295
4	USML-2	D	6	*A*	188	*B*	59	*B*	246	*B*	295
5	USML-2	D	20	*A*	67	*B*	21	*B*	85	*B*	257
6	LMS	D	20	*A*	188	*B*	59	*B*	246	*B*	295
7	LMS	D	20	*A*	188	*B*	59	*B*	246	*B*	295
8	USML-2	FID	7	H_2O	470	None	None	*A*	235	*B*	598
9	USML-2	FID	17	H_2O	470	None	None	*A*	235	*B*	598
10	USML-2	FID	35	H_2O	470	None	None	*A*	235	*B*	598
11	LMS	FID	35	H_2O	470	None	None	*A*	235	*B*	598
12	LMS	FID	100	H_2O	470	None	None	*A*	235	*B*	598

an actual space mission were evaluated in a maiden experiment on SpaceHab-01 during the IML-2 mission in 1994 (Riès-Kautt *et al.*, 1997).

The APCF was activated on both the USML-2 mission and the LMS mission several hours after a microgravity environment had been achieved, and deactivated (the stopcocks rotated in reverse) a few hours before re-entry. The duration of activation of the crystallization reactors under the microgravity environment was 14 d for the USML-2 mission and 16 d for the LMS mission. In the case of the dialysis cells, parallel experiments were carried out in Strasbourg in identical reactors during the periods of both missions. No parallel ground controls were carried out for the free-interface diffusion reactors because turbulence due to convective mixing at the interface profoundly affects the manner and kinetics by which supersaturation is attained in the system. Thus, the method functions quite differently in a 1*g* environment. Following the missions, the dialysis cells were returned to Strasbourg for analysis, while the free-interface diffusion cells were sent to Riverside. They were, in both cases, examined immediately and photographed, and X-ray diffraction analyses were initiated.

2.3. *Crystallographic methods*

Crystallographic analyses using conventional X-ray sources were performed immediately after recovery of the space-grown crystals. Synchrotron studies were performed as soon as beam time became available (no measurements were made on crystals, either from space or grown on earth, older than four months).

At Riverside, complete three-dimensional X-ray diffraction data were collected at 290 K for the crystals grown on USML-2 by free-interface diffusion, as described previously (Ko, Ng & McPherson, 1993; Ko, Ng, Day, Greenwood & McPherson, 1993; Larson *et al.*, 1993). Data were collected from capillary-mounted crystals using a San Diego Multiwire Systems (SDMS) double multiwire detector system (Xuong, Nielson, Hamlin & Anderson, 1985) with crystal-to-detector distances of 900 and 838 mm. Frame sizes were 0.10° with 2.5 min per frame. The X-rays were generated by a Rigaku RU-200 rotating-anode generator operated at 45 kV and 135 mA with a Supper monochromator to give radiation of 1.54 Å wavelength. Crystals were exposed for 24–48 h. Data-collection procedures and experimental parameters were identical for both the earth- and the space-grown crystals. Redundancy of recordings ranged from four to eight. Data correction, reduction, merging and statistical analysis were performed using the programs supplied by SDMS. For both earth- and microgravity-grown crystals, the R_{sym} values varied from 0.035 to 0.06 in the outside shells of data for reflections having $I/\sigma > 3$.

Three-dimensional X-ray data were collected by the Strasbourg group at the EMBL Outstation DESY, Hamburg, Germany, on beamline X11 using a MAR Research image plate. Complete data sets for thaumatin crystals grown on LMS and for the corresponding earth-grown control crystals were obtained using crystals of the same size and the same volume. Data were collected at 293 K with a crystal-to-detector distance of 250 mm. Oscillation angles of 0.5° were used with an X-ray wavelength of approximately 0.91 Å; the exposure time varied between 20 and 30 s. Data collection was evaluated on-line with the programs *DENZO* and *SCALEPACK* (Otwinowski & Minor, 1996) at the DESY synchrotron station. Data for both earth- and microgravity-grown crystals were collected to 1.6 Å with R_{sym} values ranging from 0.021 to 0.175 to the limits of resolution of the data set for reflections having $I/\sigma > 3$.

The mosaicities of the thaumatin crystals, obtained under both earth and space growth conditions, were

evaluated by measuring the rocking widths for selected reflections presented as the full width at half maximum (FWHM) (Helliwell, 1988). Crystal mosaicity yields the angular dispersion of the crystal blocks charaterizing the crystals and, in turn, reflects the intrinsic crystal order (Weisgerber & Helliwell, 1993). Space- and earth-grown crystals of the same volume were mounted in standard glass capillaries of 0.5 mm diameter. Data for mosaicity measurements were recorded by using a CCD detector on beamline CRG BM2 (D2AM) at ESRF, Grenoble, France. This particular synchrotron beamline produces highly collimated intense radiation of very low divergence and minimal $\delta\lambda/\lambda$. The critical energy was 19.5 keV with a focused beam of 0.3 mm diameter at the sample and with a maximum vertical divergence of 0.15 mrad and a maximum horizontal divergence of 9.0 mrad (Ferrer, Hirschler, Roth & Fontecilla-Camps, 1996). The intensity of the full beam was about 10^{11} photon s^{-1} at 0.98 Å wavelength, with an energy resolution, $\delta\lambda/\lambda$, of approximately 10^{-4}. Direct monochromatic measurements were obtained by recording data over oscillation ranges of 0.5° for indexing of reflections and subsequently at an oscillation angle of 0.003°, with 0.2° crystal rotation at 10 s exposure per frame. The data for mosaicity analysis were processed with *XDS* and images of the intensities generated and quantitated with *MARVIEW* (Kabsch, 1988*a*,*b*).

Reflections were measured in the vertical plane with respect to the direct beam so that a fully recorded reflection can be expressed as

$$\varphi_r = \gamma + \eta + (\delta\lambda/\lambda)\tan\theta,$$

where φ is the reflecting range, γ is the mean divergence in the plane defined by the direct and the diffracted beams, η is the crystal sample mosaicity, λ is the average wavelength of the X-ray beam and θ is the Bragg angle of the reflection (Snell *et al.*, 1995; Ferrer *et al.*, 1996). The values of γ and $\delta\lambda/\lambda$ were minimized in this study by considering only reflections located in the vertical plane including the incident beam and those at low resolution. The measured FWHM has the value of the instrument resolution function, IRF (0.15 mrad or 0.009°), deconvoluted out. The profiles presented here were not corrected for Lorentz broadening.

3. Results and discussion

3.1. *The protein model*

Thaumatin is a monomeric protein from the African Serendipity berry (*Thaumatococcus daniellii*) and is valued for its intensely sweet taste and its use as a non-caloric sweetener. It has a molecular weight of 21 500, contains four disulfide bridges and possesses a high degree of stability. It consists primarily of β structure organized in two associated domains. The structure was first determined in an orthorhombic crystal form at 1.7 Å resolution (Ogata, Gordon, de Vos & Kim, 1992), and later in a second orthorhombic, a monoclinic and a tetragonal crystal form (Ko, Day, Greenwood & McPherson, 1994). The tetragonal crystal form, grown from tartrate and refined to 1.7 Å resolution (Ko, Day, Greenwood & McPherson, 1994), was studied in these experiments. The mechanisms and kinetics of growth at the molecular level for thaumatin crystals are among the most thoroughly characterized of any protein crystal (Malkin, Kuznetsov & McPherson, 1996; Malkin, Kuznetsov, Glantz & McPherson, 1996). Crystals can be grown in a conventional laboratory in 12–48 h at room temperature by a variety of methods. The crystals are in space group $P4_12_12$ with $a = b = 59$ and $c = 158$ Å; there is a single molecule in the asymmetric unit. The habit is that of a tetragonal bipyramid, often reaching linear dimensions greater than 1 mm. The crystals, which contain about 45% solvent, are mechanically robust. Their growth has been studied by a variety of physical techniques, including interferometry (Kuznetsov, Malkin, Greenwood & McPherson, 1995) and atomic force microscopy (Malkin, Kuznetsov & McPherson, 1996; Malkin, Kuznetsov, Glantz *et al.*, 1996).

3.2. *Visual and microscopic observations*

For both missions, crystals were observed in all of the reactors (both the dialysis and the free-interface diffusion reactors) returning from space. All of the dialysis reactors activated as ground controls for both missions also contained crystals. There was a clear increase in the average and largest sizes of crystals grown by dialysis in microgravity compared with the ground control crystals, as seen in Table 2 and Figs. 1 and 2. In the best of the three free-interface diffusion reactors, the largest crystals, seen in Fig. 3, were three to five times the volume of the best crystals produced in either laboratory on earth. In both cell types, some of the largest thaumatin crystals measured more than 2 mm from apex to apex of the tetragonal bipyramids.

The number and sizes of crystals from the dialysis reactors were assessed with an optical microscope; the results are summarized in Table 2. Each of the flight reactors contained 30 to 250 crystals having a size range of 0.4–1.8 mm. The corresponding ground control reactors contained approximately 550 to more than 1000 crystals, in the size range 0.1–0.9 mm. Fig. 1 presents representative photographs of the microgravity-grown crystals compared with the corresponding earth-grown crystals.

A notable observation originating independently from both the Strasbourg group (using dialysis) and the Riverside group (using free-interface diffusion) was the dependence of the average and largest sizes on protein concentration, a fundamental experimental variable. Independent of approach, the largest crystals consistently grew at the highest protein concentration and the smallest

Table 2. *Number and size of space- and earth-grown crystals in APCF dialysis reactors*

Reactors 1–5 were on USML-2 and 6 and 7 were on LMS. Even though reactors flown on LMS contained many crystals from space as well as on the ground, it was qualitatively observed that the space-grown crystals were fewer in number and larger than those grown on earth. Reactors containing more than 1000 crystals are denoted 1000+; the number of crystals exceeding 1000 could not be counted with high accuracy therefore a precise number is not given.

Reactor (protein chamber size, μl)	Space		Corresponding earth control	
	No. of crystals	Average size (longest dimension, mm)	No. of crystals	Average size (longest dimension, mm)
1 (67)	30	1.5	550	0.8
2 (188)	150	0.6	1000+	0.1
3 (188)	50	0.6	1000+	0.1
4 (188)	275	0.5	1000+	0.1
5 (188)	150	0.5	1000+	0.1
6 (188)	1000+	0.4	1000+	0.3
7 (188)	1000+	0.4	1000+	0.3

crystals at the lowest protein concentration. This is shown in Fig. 3 for crystals grown at three different protein concentrations (7, 17 and 35 mg ml^{-1}) by free-interface diffusion under otherwise identical conditions.

Visually, the quality of the crystals, particularly those growing free of any surfaces, and including the largest, was very high. They appeared virtually flawless, with no observable imperfections, striations or habit anomalies. Crystals attached to the cell walls (which presumably nucleated there) did show defects near the sites of growth initiation but became flawless as growth proceeded into the bulk solution.

3.3. *X-ray intensity measurements*

X-ray diffraction data were collected from a total of four thaumatin crystals grown in microgravity by free-interface diffusion. The data were merged to form a single data set. This microgravity set was then compared with the best data previously obtained from crystals grown in a conventional laboratory, data which were, in fact, used to solve and refine the reported structure of the tetragonal thaumatin crystals (Ko *et al.*, 1994). This comparison is shown in Fig. 4(*a*), where average intensity divided by estimated error is presented as a function of resolution expressed as $\sin^2\theta/\lambda^2$. As with several previously reported investigations of macromolecular crystal growth in microgravity, two features of the comparison emerged. First, the I/σ ratio of reflections obtained for crystals grown in microgravity was higher than (approximately double) that for earth-grown crystals over the entire resolution range analysed. Second, the limit of resolution of the diffraction pattern was higher for microgravity-grown crystals than for crystals grown on earth: 1.5 *versus* 1.7 Å resolution, respectively. While 0.2 Å may appear only a marginal increase, in this portion of the resolution range it is significant and, combined with the improved I/σ over the entire resolution range, yields nearly 30% more diffraction

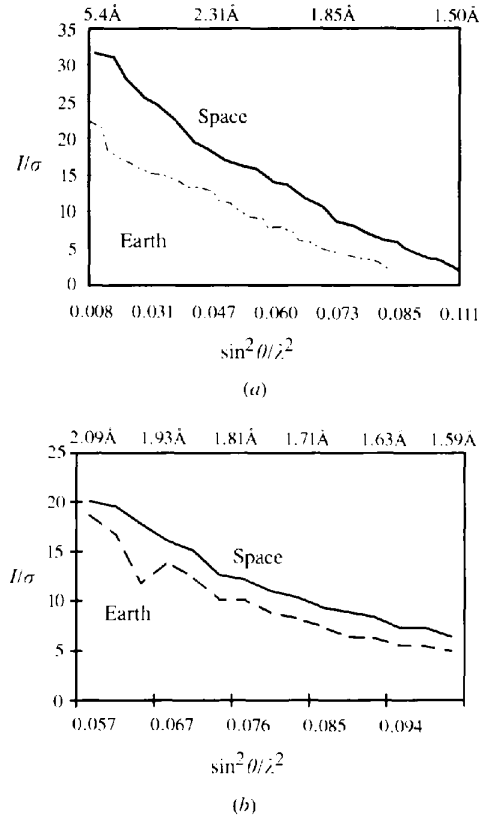

Fig. 4. Graphs of the intensity (I) *versus* estimated error (σ) ratio as a function of resolution ($\sin^2\theta/\lambda^2$) for thaumatin earth- and space-grown crystals analysed by (*a*) conventional and (*b*) synchrotron sources. The graphs are presented as modified I/σ *versus* resolution plots where the value of I/σ is the effective 'signal-to-noise' ratio for the diffraction pattern at the resolution corresponding to the respective $\sin^2\theta/\lambda^2$ value. For the resolution range shown, space-grown crystals yield as much as 30% more diffraction intensities ($> 3\sigma$) than the best crystals grown on earth. Crystals analysed in the Riverside Laboratory were from (*a*) free-interface diffusion reactors and those examined under synchrotron radiation were from (*b*) dialysis reactors, all flown on the LMS mission. The limit of resolution for the crystals analysed with a synchrotron source was not measured.

intensities ($> 3\sigma$) for the microgravity-grown crystals. We would like to point out that the true limit of resolution for the microgravity-grown crystals was never measured during this analysis because technical constraints prevented collection of data beyond 1.5 Å. The continued strength of the diffraction pattern at the 1.5 Å mark suggested to us that the actual resolution limit of the microgravity-grown crystals was beyond this point.

In another series of experiments we evaluated the diffraction properties of crystals grown in dialysis APCF cells during the LMS mission. We compared individual crystals grown in space and on earth in similar APCF cells. In all measurements, the amount of data with $I > 3\sigma$ (the average I/σ in all resolution ranges) was better for the microgravity-grown crystals than for the earth controls. Both earth- and space-grown crystals diffract easily beyond 1.6 Å; the space-grown crystals show an inclination to diffract to higher resolution. A quantitative comparison in the high-resolution range, 2.1–1.6 Å, of a representative crystal from space and one from earth, having the same size and volume, is shown in Fig. 4(*b*). The data show, reproducibly, a significant increase of the I/σ ratio for space-grown crystals over the entire resolution range investigated. This conclusion is consistent with that deduced from similar measurements, as presented in Fig. 4(*a*), that were performed on free-diffusion-grown crystals during the USML-2 mission.

3.4. *Mosaicity measurements*

Fig. 5 presents typical mosaicity profiles of three representative reflections from both space- and earth-grown crystals obtained in the frame of the LMS experiment (broken lines). The reflection profiles lie in the vertical plane of diffraction at approximately 4 Å resolution and their intensities were normalized for direct comparison. The curves appear coarse, displaying numerous shoulders, particularly in the later portions of the profiles (Figs. 5*a* and 5*b*). Such irregularities were present for all reflections, suggesting that the local features of the profile could reflect the intrinsic properties of the crystal.

Each set of reflection profiles of the space- and earth-grown crystals were averaged and Gaussian fits of the sets of profiles were calculated (solid lines). FWHM values of the Gaussian curves were measured; the FWHM was 47 millidegrees (0.047°) for a crystal grown on earth (Fig. 5*a*) compared with 10 millidegrees for the space-grown crystal (Fig. 5*b*).

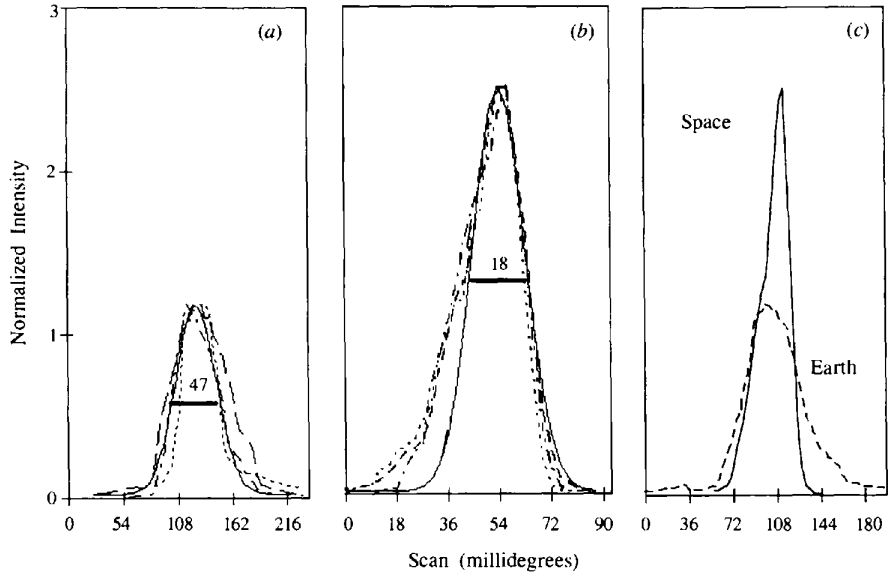

Fig. 5. Profiles of three representative reflections, $(17,\bar{1},23)$, $(\bar{2},12,12)$ and $(16,\bar{1}0,5)$, at 4 Å were evaluated from (*a*) earth- and (*b*) space-grown thaumatin crystals from the LMS experiment. Reflections were obtained in the vertical diffraction plane such that the rotation axis was horizontal and perpendicular to the X-ray beam. Each set of reflection profiles for space- and earth-grown crystals were averaged and Gaussian fits of the sets of profiles were calculated (solid lines). The Gaussian plots were fitted to the principle peaks, for which the FWHM values were obtained. Only the principle peak is considered to represent the actual mosaicity profile for space-grown crystals. The FWHM of a Gaussian fit for each profile was measured and its value deconvoluted out by the value of the instrument resolution function, IRF (0.15 mrad or 0.009°). FWHM values are indicated by short horizontal lines in the profiles; they show that the space-grown crystals are about two and a half times less mosaic than the earth-grown crystals. The intensities shown are normalized and the actual peak intensities were measured to 250 000 counts per 0.1 s for the space-grown crystal. In contrast, the spot intensities corresponding to the same reflections for the earth-grown crystal were approximately two times less. Part (*c*) shows a relative comparison of the averaged mosaicity profiles for an earth- and a space-grown crystal for the same reflections.

Notably, in all the crystal mosaicity profiles for all the analysed reflections of the space-grown crystals, a principle shoulder is observed at the beginning of the profiles, while the end of the profile remains very smooth and the curve diminishes sharply. We have no clear explanation for this observation. It may be possible that these shoulders are indicative of some degree of twinning in the crystal, or are caused by other defects not detected by low-magnification visual microscopy, produced during storage or transport on the ground. This phenomenon contributes to the nonsymmetrical fit of the Gaussian curves. In our measurements, the Gaussian plots are fitted to the principle peaks, for which the FWHM values were determined. Here, we have considered only the principle peak to represent the actual mosaicity profile for the space-grown crystals. Even if shoulder widths were included in the measurement of the FWHM, the value would still be significantly less than that of the earth-grown crystals.

Consistently, reflections from crystals grown in microgravity during both space missions displayed narrower peaks of greater amplitude compared with those of earth-grown crystals. This is likely to be a consequence of reduced discrete defects and dislocations compared with crystals grown on earth. The relative intensities and peak width differences of the averaged profiles measured for reflections derived from space- and earth-grown crystals presented in Fig. 5 typify the mosaicity of thaumatin crystals obtained on earth and in space. Table 3 summarizes the mosaicity evaluations of the space- and earth-grown crystals.

Table 3. *Mosaicity characteristics of earth- and space-grown thaumatin crystals*

Crystals labelled Space 1 were retrieved from reactor No. 6 and those labeled Space 2 from reactor No. 7. Control crystals Earth 1 and Earth 2 were prepared in parallel with crystals Space 1 and Space 2, in identical reactors and with the same solutions. The presented FWHM values have the instrument-resolution-function value deconvoluted out.

Crystal	Earth 1	Earth 2	Space 1	Space 2
FWHM (millidegrees)	54	47	21	18
Deviation (millidegrees)	5	5	3	5
Number of spots	5	3	5	3

4. Conclusions

The results presented here for thaumatin crystals grown in microgravity in the APCF by two different techniques are consistent. They reinforce the conclusion of other reports based on different macromolecules that a microgravity environment can provide unique advantages (Giegé, Drenth, Ducruix, McPherson & Saenger, 1995). In these experiments, the best crystals found in relatively few microgravity-grown samples were compared with the best crystals obtained in many thousands of ground-based trials. Thus, on a purely statistical basis, the conventional laboratory results are highly favored. Yet the microgravity-grown crystals were consistently and significantly larger, and substantially more defect free as judged by direct visual inspection. In this investigation, this appears to be independent of the choice of crystallization method and the loading and handling of the APCF cells.

An interesting observation was the clear correlation between ultimate crystal size and protein concentration. We observed in both the dialysis and the free-interface diffusion reactors in space that larger crystals were obtained at increasingly higher protein concentrations. On earth, developing protein crystals are continuously exposed to the full concentration of protein in the bulk solvent. Because of convective mixing, excessive and unfavorable supersaturation prevails throughout growth. In the absence of gravity, there is no convective mixing and thus solute transport is entirely dominated by diffusion (Pusey, Witherow & Nauman, 1988).

Because of the large size of the protein molecules and their low diffusivity, concentration gradients form in the neighborhood of the growing crystal. Without convection, these gradients, or depletion zones, are quasi stable in microgravity (Koszelak, Leja & McPherson, 1996). In these circumstances, the crystals are exposed to nutrient solutions of reduced supersaturation. The process of macromolecular crystal growth in microgravity is, in a sense, self-regulating. This idea may explain the observations presented here which show, both qualitatively and quantitatively, that under a microgravity environment crystal growth is improved compared with crystal growth on earth.

The results presented here suggest that in future experiments larger crystals of higher quality may be obtained by even further increasing the concentration of the macromolecule compared with that utilized in conventional laboratories. This is contrary to what one would do generally in the conventional laboratory, where the best results are usually achieved at the lowest levels of supersaturation.

The resolution limit of the diffraction pattern, the I/σ ratio as a function of the Bragg angle, and the mosaic spread of crystals are generally agreed to reflect both the degree of internal order and the long-range defect structure and its distribution within the crystal. That is, they serve as measures of the average statistical disorder of the molecules about the lattice points, as well as of the extent of local but severe disorder introduced by defects such as dislocations, stacking faults, point defects or incorporated foreign material (Malkin, Kuznetsov & McPherson, 1996). All of the data presented here, both intensity distributions and mosaic spread measurements, imply a higher degree of internal order, a lower defect density and a reduction of severe faults for crystals grown in the absence of gravity.

While similar results based on intensity data for microgravity-grown crystals of several proteins have

been reported previously (DeLucas *et al.*, 1989; Day & McPherson, 1992; Koszelak *et al.*,1996), and comparable results based on mosaicity measurements have been presented for other crystals (Snell *et al.*, 1995), this is the first experiment to produce crystals grown by multiple methods and analysed by both approaches. Indeed, our conclusion is that they are mutually supportive and complementary, and both suggest the same conclusion, *i.e.* that crystals grown in microgravity show significantly improved diffraction properties when compared with crystals grown on earth.

Apart from lysozyme, no other protein crystal has been used to investigate mosaicity differences between earth-grown and space-grown crystals. The data presented here indicate that the mosaic spread of reflections from microgravity-grown thaumatin is reduced by more than a factor of two relative to that of earth-grown crystals. This is comparable to observations of tetragonal lysozyme, space-grown crystals of which showed an improvement by a factor of three over the corresponding earth controls (Ferrer *et al.*, 1996; Snell *et al.*, 1995).

Thaumatin crystals grown on earth may be composed of multiple mosaic blocks, represented by shoulders in the profiles which can be decomposed into unresolved minor peaks. Substructures of a mosaic crystal could contribute to the individual peaks and such substructural components in single crystals may be a consequence of crystal growth dislocations. The density of these dislocations is not uniform as they tend to group themselves into cell (subgrain) boundaries (Rosenberger, Muschol, Thomas & Vekilov, 1996). This is indicated by the monochromatic X-ray topographs of hen egg-white lysozyme, which show fluctuating rocking width profiles corresponding to the disorientation of subgrains (Fourme, Ducruix, Riès-Kautt & Capelle, 1995). In the case of thaumatin, atomic force microscopy (AFM) studies have shown that crystals exhibit a variety of defects, including unoccupied lattice sites, linear defects and stacking faults (Malkin, Kuznetsov, Glantz *et al.*, 1996). The profiles shown in Fig. 5 typify the mosaic spread obtained from all control crystals analysed; their irregular profiles may reflect the ensemble of defects characteristic of earth-grown crystals. The Gaussian fits of representative space-grown-crystal reflection profiles have average FWHM values about four times less than those of earth-grown crystals (Fig. 5*b*). In contrast to profiles from earth-grown crystals, those from the space-grown crystals are smoother and more intense, and display narrower peaks.

Even though the majority of other microgravity studies reported are for the most part very positive, it has not been clear whether microgravity can positively influence crystal growth for all proteins. It is fair to say that not all microgravity experiments share the same conclusion (Erdmann *et al.*, 1989; Hilgenfeld, Liesum, Storm & Plaas-Link, 1992; Stoddard, Strong, Arrott & Farber, 1992). For example, it could be shown for crystals grown during the unmanned COSIMA-2 mission that space-grown crystals of *Streptomyces coelicolor* lysozyme and *Bacillus thermoproteolyticus* were of worse quality than the ground controls (Hilgenfeld *et al.*, 1992). However, as pointed out by the researchers, their observations are not conclusive generally, but could reflect specific features of the particular proteins they studied. In addition, conclusions of past crystal growth studies in microgravity environments have often been complicated by a lack of ground controls or limited quantitative analytical procedures. Because the geometry and design of the crystallization vessels, the quality of the samples, and the overall motion of the crystallization system are critical factors affecting crystallization processes, we have made great efforts to study our space results with respect to direct parallel ground controls based on the APCF dialysis reactors. We emphasize in this study that space-grown crystals were not only compared with the best earth data but also to crystals obtained from parallel ground reactors treated, as far as possible, in an identical manner to their space counterparts. Moreover, we have used two different types of crystal-growth vessels, each providing different growth conditions, and have evaluated our results by examining the intensities of each crystal as a function of resolution and the mosaic spread of the crystal.

The general conclusion for thaumatin crystal growth, in all cases reported here, is that microgravity provides better looking crystals of higher crystallographic quality, regardless of containment types or concentration variances in the crystallization set-ups.

This research was supported by grants from the National Aeronautics and Space Administration (NASA), the Centre National d'Etudes Spatiales (CNES) and the Centre National de la Recherche Scientifique (CNRS). We acknowledge the help of Philippe Dumas, A. Théobald-Dietrich and C. Sauter at various stages of this project in Strasbourg. We thank J. R. Helliwell and J. Hirschler for discussions on mosaicity. We are grateful to R. Bosch and P. Lautenschlager at Dornier GmbH for their technical support. We thank DESY at Hamburg and ESRF at Grenoble for the provision of synchrotron facilities. We acknowledge M. Roth (Grenoble) for his assistance. Our appreciation also extends to the European Space Agency (ESA) for flight opportunities on the NASA space shuttle and K. Fuhrmann and O. Minster of ESA for their administrative support. Finally, we thank CNES for a fellowship awarded to JDN.

References

Asano, K., Fujita, S., Senda, T. & Mitsui, Y. (1992). *J. Cryst. Growth*, **122**, 323–329.

Bosch, R., Lautenschlager, P., Potthast, L. & Stapelmann, J. (1992). *J. Cryst. Growth*, **122**, 310–316.

Chayen, N. E., Gordon, E. J. & Zagalsky, P. F. (1996). *Acta Cryst.* D**52**, 156–159.
Day, J. & McPherson, A. (1992). *Protein Sci.* **1**, 1254–1268.
DeLucas, L. J., Smith, C. D., Smith, H. W., Senadhi, V. K., Senadhi, S. E., Ealick, S. E., Bugg, C. E., Carter, D. C., Snyder, R. S., Weber, P. C., Salemme, F. R., Ohlendorf, D. H., Einspahr, H. M., Clancy, L., Navia, M. A., Mckeever, B., Nagabhushan, T. L., Nelson, G., Babu, Y. S., McPherson, A., Koszelak, S., Stammers, D., Powell, K. & Darby, G. (1989). *Science*, **246**, 651–654.
Erdmann, V. A., Lippmann, C., Betzel, C., Dauter, Z., Wilson, K., Hilgenfeld, R., Hoven, J., Liesum, A., Saenger, W., Müller-Fahrnow, A., Hinrichs, W., Düvel, M., Schulz, G. E., Müller, C. W., Wittmann, H. G., Yonath, A., Weber, G., Stegen, K. & Plaas-Link, A. (1989). *FEBS Lett.* **259**, 194–198.
Ferrer, J.-L., Hirschler, J., Roth, M. & Fontecilla-Camps, J. C. (1996). *ESRF Exp. Rep.* pp. 27–28.
Fourme, R., Ducruix, A., Riès-Kautt, M. & Capelle, B. (1995). *J. Synchrotron Rad.* **2**, 136–142.
Giegé, R., Drenth, J., Ducruix, A., McPherson, A. & Saenger, W. (1995). *Prog. Cryst. Growth Charact.* **30**, 237–281.
Helliwell, J. R. (1988). *J. Cryst. Growth*, **90**, 259–272.
Helliwell, J. R., Snell, E. & Weisgerber, S. (1996). *Materials & Fluids Under Low Gravity, Lecture Notes in Physics*, edited by L. Ratke, H. Walter & B. Feuerbacher, pp. 155–170. Berlin: Springer-Verlag.
Hilgenfeld, R., Liesum, A., Storm, R. & Plaas-Link, A. (1992). *J. Cryst. Growth*, **122**, 330–336.
Kabsch, W. (1988*a*). *J. Appl. Cryst.* **21**, 67–71.
Kabsch, W. (1988*b*). *J. Appl. Cryst.* **21**, 916–924.
Ko, T.-P., Day, J., Greenwood, A. & McPherson, A. (1994). *Acta Cryst.* D**50**, 813–825.
Ko, T.-P., Ng, J. D., Day, J., Greenwood, A. & McPherson, A. (1993). *Acta Cryst.* D**49**, 478–489.
Ko, T.-P., Ng, J. D. & McPherson, A. (1993). *Plant Physiol.* **101**, 729–744.
Koszelak, S., Day, J., Leja, C., Cudney, R. & McPherson, A. (1995). *Biophys. J.* **69**, 13–19.
Koszelak, S., Leja, C. & McPherson, A. (1996). *Biotech. Bioeng.* **52**, 449–458.
Kuznetsov, Yu. G., Malkin, A. J., Greenwood, A. & McPherson, A. (1995). *J. Struct. Biol.* **114**, 184–196.
Larson, S. B., Koszelak, S., Day, J., Greenwood, A., Dodds, A. & McPherson, A. (1993). *J. Mol. Biol.* **231**, 375–391.
Long, M. M., Bishop, J. B., Nagabhushan, T. L., Reichert, P., Smith, G. D. & DeLucas, L. J. (1996). *J. Cryst. Growth*, **168**, 233–243.
Malkin, A. J., Kuznetsov, Yu. G., Glantz, W. & McPherson, A. (1996). *J. Phys. Chem.* **100**, 11736–11743.
Malkin, A. J., Kuznetsov, Yu. G. & McPherson, A. (1996). *J. Struct. Biol.* **117**, 124–137.
Ogata, C. M., Gordon, P. F., de Vos, A. M. & Kim, S. H. (1992). *J. Mol. Biol.* **3**, 893–908.
Otwinowski, Z. & Minor, W. (1996). In *Methods in Enzymology*, Vol. 276, edited by C. W. Carter Jr & R. M. Sweet. New York: Academic Press.
Pan, J.-S., Niu, X.-T., Gui, L.-L., Zhou, Y.-C. & Bi, R.-C. (1996). *J. Cryst. Growth*, **168**, 227–232.
Pusey, M., Witherow, W. K. & Nauman, R. (1988). *J. Cryst. Growth*, **90**, 105–111.
Riès-Kautt, M., Broutin, I., Ducruix, A., Shepard, W., Kahn, R., Chayen, N., Blow, D., Paal, K., Littke, W., Lorber, B., Théobald-Dietrich, A. & Giegé, R. (1997). *J. Cryst. Growth.* In the press.
Rosenberger, F., Muschol, M., Thomas, B. R. & Vekilov, P. G. (1996). *J. Cryst. Growth*, **168**, 1–27.
Snell, E. H., Weisgerber, S., Helliwell, J. R., Weckert, E., Hölzer, K. & Schroer, K. (1995). *Acta Cryst.* D**51**, 1099–1102.
Snyder, R. S., Fuhrmann, K. & Walter, H. U. (1991). *J. Cryst. Growth*, **110**, 333–338.
Stoddard, B. L., Strong, R., Arrott, A. & Farber, G. F. (1992). *Nature (London)*, **360**, 293–294.
Weisgerber, S. & Helliwell, J. R. (1993). *Jnt CCP4 ESF-EACBM Newslett. Protein Crystallogr.* **29**, 10–13.
Xuong, N.-H., Nielson, C., Hamlin, R. & Anderson, D. (1985). *J. Appl. Cryst.* **18**, 342–360.